Interpretation of the small-strain moduli of model networks of polydimethylsiloxane

M. A. Sharaf*
Department of Chemistry, United Arab Emirates University, Box 17551, Al Ain, United Arab Emirates

and J. E. Mark†
Department of Chemistry and the Polymer Research Center, The University of Cincinnati, Cincinnati, OH 45221, USA
(Received 10 June 1993)

Small-strain moduli reported in the literature for polydimethylsiloxane (PDMS) model networks have been critically re-examined, with account being taken of recent studies which have demonstrated the occurrence of significant side reactions in hydrosilylations. When the effects of such side reactions on network structure parameters are properly taken into account, the elasticity results can be well explained using the recent molecular theory of Flory and Erman. The revised calculations show a transition in the modulus from the affine to the phantom limit of deformation as the degree of chemical crosslinking increases. This is to be expected when the constraints on the fluctuation of junctions vanish (because of the decreased interspersion of chains), and such constraints are expected to vanish even in the small-strain region when the chains are sufficiently short. In lieu of carefully controlled reactions with well-defined stoichiometries, it appears that the procedure best suited for testing the various theories of rubber-like elasticity is a plot of the modulus G (as approximated by the sum $2C_1+2C_2$ of the Mooney–Rivlin constants) against the phantom modulus $[f^*]_{ph}$ (as approximated by $2C_1$). Also of importance is the difference between the 'effective' number of network chains ν (relevant to theory) and the commonly used 'active' number of chains ν_a.

(Keywords: polydimethylsiloxane; elastomers; networks)

INTRODUCTION

In recent years, a considerable number of studies have been carried out on model networks of polydimethylsiloxane (PDMS). A central goal of these studies is to test the applicability of the various theories of rubber-like elasticity. By employing end-linking reactions, the number of strands between junctions and the functionalities of the junctions can be controlled. These techniques usually involve the reaction between bifunctionally terminated polymer chains and multifunctional end-linking agents having a functionality $\varphi \geqslant 3$.

The traditional theories of rubber-like elasticity have been developed on the basis of network chains being simple Gaussian random coils. Models of elastomers in the 'phantom' network limit (in which the chains are assumed to be devoid of material properties) were first developed by James and Guth[1]. The term phantom was used to emphasize that the configurations available to each network chain depend only on the position of its ends and to be otherwise independent of the configurations of neighbouring chains with which they share the same region of space. In such a phantom network, it is assumed that crosslinking does not influence the distribution of end-to-end distances in the undeformed state, that the chains move freely through one another, and that the only contribution to the elasticity of the network is from the network connectivity. James and Guth[1] assumed also that the network is connected to a set of fixed surface junctions that preserve its volume. Junctions inside the elastomer are free to fluctuate around their well-defined, mean (time-averaged) positions. Fluctuations of the junctions are strain independent, whereas all the time-averaged vectors transform affinely with applied macroscopic strain. The theory has been successful in many respects, but some aspects of stress–strain behaviour differ significantly from its predictions.

In an affine network[2–4], on the other hand, the end-to-end chain vectors are assumed to transform affinely (linearly) with macroscopic deformation. Fluctuations of the junctions are completely suppressed by local intermolecular entangling with neighbouring chains sharing the same region of space.

The role of trapped entanglements on the mechanical properties at equilibrium has been the subject of conflicting opinions[5–36]. Macosko and co-workers[5–12], Ferry[13], Langley[14], Graessley and co-workers[15,16], Merrill and co-workers[17–19], Opperman and Rennar[20], and Edwards[21] have argued that in the limit of small strains, trapped entanglements contribute to the modulus. This is thought to be due to the large amount of overlap existing in the domains pervaded by neighbouring strands

* Permanent address: Department of Chemistry, Cairo University at Beni-Suef, Beni-Suef, Egypt
† To whom correspondence should be addressed

0032-3861/94/04/0740–12

wherein chains cannot pass through the contours of other chains[13–16]. Hence, it follows that the configurations of neighbouring chains may well depend on one another, producing additional contributions to the partition function[13–16]. In other words, discrete entanglements consisting of well-defined loops of one chain about another are thought to act as crosslinks between the chains thus entwined. If the chains are crosslinked, it can be argued that a portion of the interaction that contributed to the plateau modulus will not relax out and, thus, will increase the network modulus[13–16]. Interpretation of a comprehensive array of data confined to the region of small strain, has led many investigators to argue, compellingly, that in this region discrete (trapped) entanglements are present along the chain contours and contribute directly to the modulus[5–21].

The phantom and affine limits of deformation are two extreme cases, and experimental stress–strain measurements suggest that real networks exhibit properties between these two limits[1,4,32–36]. The suggestion of a gradual transition between affine and phantom limits with increasing deformation, in terms of decreasing intermolecular entanglements among the chains, was first suggested by Ronca and Allegra[32]. More recently, a comprehensive molecular theory for real networks based on this idea was formulated by Flory and Erman[33–36]. One of the major premises of the theory is that local intermolecular entanglements and steric constraints on the fluctuations of junctions contribute to the modulus at intermediate deformations. It was emphasized that the constraints on junctions are due to 'diffuse' elastic entanglements of chains with their neighbours, and are diminished by swelling[33–36]. In further elaboration, the chains pendent at a given junction must adopt configurations that are free of spatial overlaps with neighbouring chains and associated junctions with which they share the same region of space. Extensive interpenetration of different portions of the network that are topologically remote implies chains and junctions are inextricably involved[33–36]. Accordingly, fluctuations of the junctions about their mean positions are restricted on this account. The constraints postulated here depend on the number of eligible configurations available to the system. Therefore, they are operative at equilibrium as opposed to the discrete entanglements often proposed to interpret the time-dependent behaviour of polymers[33–36].

At least some experimental results suggest there is no significant augmentation to the large-strain modulus from trapped entanglements[22–31], and that these moduli can generally be well interpreted simply from the Flory–Erman theory[33–36]. After some of these experiments had been carried out, however, a better understanding was obtained of the hydrosilylation cure often used in the preparation of model PDMS networks. In particular, Macosko and Saam[11] used vinyl-terminated polyisobutylene to explore this issue, even though the reactions were previously considered to be straightforward and almost free of side reactions. They observed, instead, two major side reactions. The first consumes Si-H groups to give redistributed siloxane groups in the resulting polymer, as well as gaseous silanes and siloxanes as by-products. The other side reaction, on the other hand, results in a loss of reactivity of some vinyl groups owing to their shift to an internal position within the chain. These side reactions were reported to be important when experiments were conducted at high temperatures[11,37]. The maximum value of the modulus of networks prepared in this way was found to occur at a value of the stoichiometric ratio $r \approx 1.2$ (where r is the initial molar ratio of Si-H groups to vinyl groups)[5,9,38]. The effects of this stoichiometric imbalance were properly accounted for when the side reactions were taken into consideration[11].

In a number of previous studies, the maximum value of the modulus for trifunctional and tetrafunctional PDMS networks were obtained at values of r of ~ 1.1–1.3[5,9,38]. In the absence of significant side reactions, it is expected that balanced stoichiometry ($r = 1.0$) should lead to a network having complete end linking, giving the highest possible value of the modulus, and computer simulations lend support to this assumption[39]. If this is not the case, the stoichiometry in such reactions may not be accurately defined and values of the extent of reaction somewhat questionable.

In the present investigation, the theory of local constraints on junctions is used to interpret the properties of model PDMS networks. Results reported in the literature for the small-strain modulus of such networks will be re-examined, and account will be taken of the dependence of calculated values of network parameters on the hydrosilylation side reactions described recently by Macosko and Saam[11]. One of the major concerns will be the possible role played by trapped entanglements, a subject of continuing interest. The molecular basis of the various theories of rubber elasticity will be evaluated in an attempt to reconcile some differences of opinion. Factors affecting the determination of the network parameters will be discussed, namely the concentration of elastically active chains and junctions ν_a and μ_a, respectively. This includes the importance of the non-equivalence of the 'effective' number of chains ν (relevant to theory) and the commonly used 'active' number of chains ν_a.

ELASTICITY EQUATIONS

The quantity most often used to analyse elasticity results in uniaxial deformation is the reduced stress[2–4]:

$$[f^*] = f v_2^{1/3} / A^* (\alpha - \alpha^{-2}) \tag{1}$$

where f^* is the equilibrium retractive force, v_2 the volume fraction of polymer in the network during the stress–strain measurements, A^* the undeformed cross-sectional area of the sample, and α its elongation (ratio of length in the stretched state to the length in the unstretched state at the same volume).

Experimental values of $[f^*]$ for moderate values of elongation can be represented by the simple Mooney–Rivlin equation[40,41]:

$$[f^*] = 2C_1 + 2C_2 \alpha^{-1} \tag{2}$$

where $2C_1$ and $2C_2$ are constants independent of elongation. In the limit of a molecular deformation that is 'affine' (linear in the strain), the elastic equation of state for a perfect network is[5,26]:

$$[f^*]_{\text{aff}} = \nu R T v_{2C}^{2/3} \tag{3}$$

where ν is the number density of elastically effective network chains, R the gas constant, T the absolute temperature, and v_{2C} the volume fraction of polymer chains in the system being crosslinked which were successfully incorporated in the network structure.

The shear (small-strain) modulus G is then expressed by the relationship[5,26]:

$$G=\lim_{\alpha\to 1}[f^*]=2C_1+2C_2 \tag{4}$$

It is well known that values of $2C_1+2C_2$ tend to overestimate G by $\sim 5\%$[5,26]. The modulus in the phantom limit is related to the phenomenological parameter $2C_1$ by[22–36]:

$$[f^*]_{ph}=\xi RTv_{2C}^{2/3}\approx 2C_1 \tag{5}$$

where ξ is the connectivity of the network, which is related to the network degree of interlinking for a perfect network by[26,33–36]:

$$\xi=(1-2/\varphi)\nu_a \tag{6}$$

where φ is the functionality, possibly an average, of the network junctions. The 'active' number of junctions μ_a in a perfect network free of defects is given by[26]:

$$\mu_a=\left(\frac{2}{\varphi}\right)\nu_a=\left(\frac{2}{\varphi-2}\right)\xi \tag{7}$$

Experimental stress–strain measurements indicate that real networks generally exhibit properties between the phantom and affine limits[32–36]. According to the recent theory of network behaviour by Flory and Erman, the elastic force is taken to be the sum of the two contributions[26,33–36]:

$$f=f_{ph}+f_c \tag{8}$$

where f_{ph} is the force predicted for a phantom network, and f_c is the contribution arising from local intermolecular entanglements and steric constraints on junction fluctuations. Hence, the expression for $[f^*]$ in the constraint theory becomes[26,33–36]:

$$[f^*]=\xi RTv_{2C}^{2/3}(1+f_c/f_{ph}) \tag{9}$$

where

$$f_c/f_{ph}=(\mu/\xi)[\alpha K(\lambda_1^2)-\alpha^{-2}K(\lambda_2^2)](\alpha-\alpha^{-2})^{-1} \tag{10}$$

Generally, the principal extension ratio λ_t is related to the axial elongation α at the prevailing volume V, which may differ from the volume V^0 in the reference state. The principal extensions λ_t relative to the state of reference are[4,34]:

$$\lambda_1=\alpha(V/V^0)^{1/3} \tag{11}$$

$$\lambda_2=\lambda_3=\alpha^{-1/2}(V/V^0)^{1/3} \tag{12}$$

and

$$K(\lambda^2)=B[\dot{B}(B+1)^{-1}+g(g\dot{B}+\dot{g}B)(gB+1)^{-1}] \tag{13}$$

$$B=(\lambda_t-1)(1+\lambda_t+\zeta\lambda_t^2)/(1+g)^2 \tag{14}$$

$$g=\lambda_t^2[\kappa^{-1}+\zeta(\lambda_t-1)] \tag{15}$$

$$\dot{B}=B\{[2\lambda_t(\lambda_t-1)]^{-1}+(1-2\zeta\lambda_t)[2\lambda(1+\lambda_t-\zeta\lambda_t^2)]^{-1}+2\dot{g}(1+g)^{-1}\} \tag{16}$$

$$\dot{g}=\kappa^{-1}-\zeta(1-3\lambda_t/2) \tag{17}$$

The theory predicts that f_c/f_{ph} decreases with increasing deformation, and that the modulus approaches the phantom limit at $\alpha\to\infty$. The relative contribution from the constraints in the limit $\alpha\to 1$ for a perfect network is predicted by the theory to be[34]:

$$f_c/f_{ph}=2/(\varphi-2) \tag{18}$$

and should therefore vanish as the functionality increases.

The more important of the two parameters is κ, which serves as a measure of the severity of the entanglement constraints relative to those in a phantom network, where such constraints are absent. The other parameter in the constrained-junction theory is ζ, which takes into account the possibly non-affine transformation of the domains of constraints with increasing deformation[26,33–36].

Previous results on PDMS networks indicate that κ is related to the phantom modulus, and consequently to the phenomenological parameter $2C_1$, by the relationship:

$$\kappa=A(2C_1)^{-1/2}v_{2C}^{2.1} \tag{19}$$

where, for a tetrafunctional network, $A=2$[36]. It has been observed, however, that A is not constant and increases with the molecular mass M_n of the primary chains and the functionality φ[26].

Following Langley[14] and Dossin and Graesley[15], the shear modulus at small strain ($\alpha\to 1$) is written as[5,15]:

$$G=\nu_a RT(1-2h/\varphi)+T_eG_e^\circ \tag{20}$$

where h is a parameter that scales departures from affine deformations of chain vectors and ranges from zero (for affine behaviour) to unity (for phantom networks). The quantity T_e is a trapping factor that represents the fraction of chains that are permanently entangled, and G_e° is the 'entanglement modulus' (often associated with the plateau modulus of the corresponding uncrosslinked polymer). The latter has been generally taken to be a measure of the topological interactions or intermolecular entangling between chains.

In this investigation, it is important to underscore the essential difference between the 'active' number of chains ν_a and junctions μ_a according to the Scanlan[42] and Case[43] definitions (commonly used for imperfect networks), and the number of 'elastically effective' chains ν and junctions μ (relevant to rubber elasticity theory). Graessley[44,45] has shown that the cycle rank of a random network is expressed by:

$$\xi=\nu_a-\mu_a \tag{21}$$

a result later generalized by Flory[46] to networks of any kind, giving the universal form:

$$\xi=\nu-\mu \tag{22}$$

It then follows that[46]:

$$[f^*]_{ph}=(\nu_a-\mu_a)RTv_{2C}^{2/3}=(\nu-\mu)RTv_{2C}^{2/3} \tag{23}$$

In a perfect network, the small-strain (affine) modulus is expressed by equation (3). In a real (imperfect) network, however[46]:

$$[f^*]_{aff}=\nu RTv_{2C}^{2/3} \tag{24}$$

It is worth noting that, in general[46]

$$\nu\neq\nu_a \tag{25}$$

As was pointed out by Flory[46], the identification of ν_a with ν is proper only for perfect networks; otherwise, it is an approximation that is legitimate for high-functionality networks. Flory has shown that the effective number of chains for imperfect networks is expressed rigorously by:

$$\nu=2\xi \tag{26}$$

Following the same arguments, Queslel and Mark[26] have shown that for an imperfect trifunctional network:

$$\mu = \mu_a/(3P-2) \tag{27}$$

$$\nu = \nu_a P/(3P-2) \tag{28}$$

where P is the extent of reaction of the crosslinking agent. In this process, both ν and μ are always larger than ν_a and μ_a when the reaction is incomplete.

NUMERICAL CALCULATIONS AND NETWORK PARAMETERS

For perfect model PDMS networks, the total number of chains ν_0 is calculated from[2-4]:

$$\nu_0 = \rho/M_n \tag{29}$$

where ρ is the bulk density, and M_n the number-average mass of the chains. Consequently, the cycle rank ξ and the total number of active junctions μ_a can be calculated from equations (6) and (7). On the other hand, if endlinking is incomplete or if the initial stoichiometric ratio r is different from unity, then[5-19]:

$$r = \frac{\varphi[A_f]_0}{2[B_2]_0} = \frac{\varphi[A_f]_0}{2\nu_0} \tag{30}$$

$$[A_f]_0 = \mu_0 = \frac{2r\rho}{\varphi M_n} \tag{31}$$

where $[A_f]_0$ and $[B_2]_0$ are the initial concentrations of the φ-functional crosslinking agent (for generating the junctions) and the bifunctional B_2 oligomer, respectively.

Macosko and Miller[7,47,48] have proposed branching theory for calculating the number of elastically active chains ν_a and junctions μ_a, as well as other structural parameters of the network from the sol fraction ω_s. The relevant formulae of the theory are discussed in greater detail elsewhere[7,47,48].

The occurrence of side reactions results in loss of Si-H groups that would otherwise form crosslinks, and thus the value of r will change[11]. The observed effective conversions in hydrosilylation cures of vinyl-terminated PDMS oligomers were derived in the same manner[11]. The observed conversions of P_{SiH} and P_{vi} and the initial value of r are given by[11]:

$$P_{SiH} = \frac{[SiH]_0 - [SiH]}{[SiH]_0} \tag{32}$$

$$P_{vi} = \frac{[vi]_0 - [vi]}{[vi]_0} \tag{33}$$

$$r = \frac{[SiH]_0}{[vi]_0} = \frac{P_{vi}}{P_{SiH}} \tag{34}$$

and the effective conversions to form crosslinks are[11]:

$$P'_{SiH} = \frac{P_{SiH} - P_Y}{1 - P_Y} \tag{35}$$

$$P'_{vi} = P_{vi} \tag{36}$$

$$r' = r(1-P_Y) = \frac{P'_{vi}}{P'_{SiH}} \tag{37}$$

where P'_{SiH} is the effective conversion of the SiH groups to crosslinks, P_Y the extent of loss of SiH groups through volatilization, P'_{vi} the effective conversion of the vinyl-terminated oligomer, and r' the effective value of the stoichiometric imbalance ratio. It is obvious from closer examination of Figures 6 and 7 in reference 9 that values of the modulus go through a maximum at $r/r' \approx 1.2$. In the absence of significant side reactions, it would be expected to occur at $r/r' = 1.0$.

In the present analysis, the network structural parameters ν_a and μ_a, the effective functionality ($\varphi_e = 2\nu_a/\mu_a$), the volume fraction of elastically effective chains v_2 and the factor T_e were all calculated from the corrected values of the sol fraction ω_s using branching theory, as outlined by Macosko and Miller[7,47,48]. Values of ξ and the corresponding phantom modulus were obtained from the sol fractions according to equations (22) and (23). Values of the effective number of junctions and chains μ and ν for trifunctional networks were obtained from equations (27) and (28), respectively. In order to account for the side reactions in the hydrosilylation cures mentioned above, the corrected values r' were used instead of r in the calculations. Values of the extent of reaction P_{SiH} and the correspondingly different structural parameters for the networks were obtained by an iterative solution of equations (A5) through (A7) in reference 7. Calculated values of the shear modulus G and the phantom modulus $[f^*]_{ph}$ were obtained from equations (24) and (23), respectively.

Analyses based on branching theory have neglected the fact that the large numbers of network imperfections generated by incompleteness of end-linking would act as diluent, even in the dry unswollen state[49]. As shown in equation (1), the values of both G and $[f^*]_{ph}$ should be reduced by $v_2^{-1/3}$ (where v_2 is the volume fraction of elastically effective chains in the network). Hence, values of G and $[f^*]_{ph}$ predicted by equations (3) and (24) would be:

$$[f^*]_{aff} = \nu RTv_{2C}^{2/3} v_2^{-1/3} \tag{38}$$

$$[f^*]_{ph} = \xi RTv_{2C}^{2/3} v_2^{-1/3} \tag{39}$$

where the factor $v_2^{-1/3}$ had not been accounted for in obtaining the reported experimental values of G and $[f^*]_{ph}$.

Values of $[f^*]_{\alpha\to 1}$ were calculated from the constrained-junction theory of Flory and Erman[33-36], using equations (5), (9) and (23). For each network, κ was obtained from equation (19), and an initial value of zero was arbitrarily assigned to ζ, as is frequently done[26]. In subsequent calculations, however, the value of ζ was varied for illustrative purposes, but the effects found were not substantial and are therefore not presented here. Values of ν and μ for trifunctional networks were obtained from equations (27) and (28). For tetrafunctional networks, values of ν_a and μ_a were determined from branching theory, and were used as approximate substitutes for ν and μ (even though it is known that they can be somewhat different).

In this connection, one should be aware that it is difficult to obtain accurate values of the sol fraction, particularly in view of the small quantities that frequently have to be measured. Nonetheless, we shall use branching theory to calculate the structure parameters of the network in that it is the best option at hand.

RESULTS AND DISCUSSION

The data collected from several studies on model PDMS networks, and previously analysed by Gottlieb *et al.*[5], are now re-examined using the scheme described above.

Table 1 Elastomeric properties of the trifunctional PDMS networks[a]

Source	M_n (g mol^{-1})	r^a	ω_s	P_{SiH}	φ	φ_e	κ	$\nu_0 RT$ (N mm^{-2})	$\nu_a RT$ (N mm^{-2})	νRT (N mm^{-2})	G (N mm^{-2})	$[f^*]_{ph}$ (N mm^{-2})	$[f^*]_{\alpha\to 1}$ (N mm^{-2})	$G/\nu RT$	$2C_1$ (N mm^{-2})	$2C_2$ (N mm^{-2})
Mark *et al.*[23]	32900	1.00	0.0300	0.890	3.0	2.8	19.4	0.000	0.032	0.042	0.067	0.013	0.028	2.10	0.033	0.034
	25600	1.00	0.0290	0.890	3.0	2.7	18.2	0.094	0.041	0.055	0.095	0.014	0.034	2.28	0.043	0.052
	18500	1.00	0.0300	0.889	3.0	2.8	15.0	0.130	0.056	0.075	0.127	0.021	0.047	2.25	0.066	0.061
	9500	1.00	0.0110	0.923	3.0	2.8	9.5	0.253	0.152	0.182	0.150	0.053	0.114	0.99	0.093	0.057
	4700	1.00	0.0300	0.889	3.0	2.7	7.9	0.512	0.221	0.295	0.159	0.075	0.152	0.72	0.148	0.011
	4000	1.00	0.0210	0.902	3.0	2.7	6.8	0.601	0.297	0.380	0.207	0.101	0.199	0.70	0.192	0.015
Meyers[19]	21600	1.00	0.0180	0.910	3.0	2.9	14.6	0.111	0.058	0.073	0.168	0.022	0.049	2.88		
	15200	1.01	0.0129	0.911	3.0	2.8	12.1	0.158	0.090	0.112	0.203	0.032	0.072	2.26		
	11100	1.00	0.0281	0.891	3.0	2.7	12.0	0.217	0.096	0.127	0.165	0.033	0.074	1.71		
	8800	1.00	0.0173	0.908	3.0	2.8	9.7	0.273	0.144	0.180	0.210	0.050	0.107	1.46		
Macosko and Benjamin[9]	39900	0.99	0.1020	0.841	3.0	2.9	27.4	0.060	0.013	0.020	0.045	0.006	0.013	3.55		
	39900	0.99	0.1030	0.841	3.0	2.9	27.8	0.060	0.012	0.020	0.053	0.006	0.013	4.25		
	30000	1.09	0.0325	0.835	3.0	2.7	19.1	0.080	0.031	0.052	0.112	0.013	0.028	3.59		
	30000	1.21	0.0358	0.777	3.0	2.4	20.6	0.080	0.027	0.064	0.097	0.011	0.025	3.60		
	30000	1.29	0.0367	0.745	3.0	2.3	20.6	0.080	0.025	0.080	0.102	0.011	0.024	4.04		
	22400	1.00	0.0760	0.851	3.0	2.6	21.8	0.107	0.028	0.043	0.061	0.010	0.024	2.16		
	22400	1.00	0.0730	0.853	3.0	2.7	21.3	0.107	0.028	0.042	0.062	0.010	0.024	2.24		
	11400	0.91	0.0790	0.899	3.0	2.8	14.6	0.211	0.058	0.075	0.065	0.022	0.047	1.12		
	11400	1.00	0.0314	0.888	3.0	2.7	12.5	0.211	0.090	0.120	0.124	0.031	0.069	1.38		
	11400	1.11	0.0073	0.863	3.0	2.6	10.6	0.211	0.121	0.178	0.193	0.042	0.095	1.59		
	11400	1.21	0.0060	0.814	3.0	2.4	11.1	0.211	0.114	0.210	0.192	0.038	0.089	1.69		
	11400	1.31	0.0040	0.775	3.0	2.3	11.1	0.211	0.111	0.265	0.221	0.038	0.088	1.99		
	11400	0.99	0.0381	0.887	3.0	2.7	12.7	0.211	0.082	0.110	0.098	0.030	0.064	1.19		
	11400	0.99	0.0369	0.888	3.0	2.7	12.9	0.211	0.085	0.113	0.096	0.029	0.065	1.14		
	11400	1.11	0.0106	0.885	3.0	2.6	11.1	0.211	0.111	0.168	0.126	0.038	0.086	1.13		
	11400	1.34	0.0055	0.759	3.0	2.3	11.7	0.211	0.103	0.281	0.182	0.035	0.081	1.77		
	5430	0.99	0.1190	0.835	3.0	2.6	12.9	0.443	0.079	0.130	0.062	0.028	0.059	0.79		
	4190	0.99	0.0497	0.876	3.0	2.6	8.5	0.574	0.196	0.273	0.147	0.065	0.133	0.75		
	4190	1.15	0.0255	0.813	3.0	2.5	7.9	0.574	0.223	0.413	0.169	0.076	0.155	0.76		
	4190	1.25	0.0418	0.757	3.0	2.3	9.1	0.574	0.170	0.474	0.125	0.057	0.120	0.73		
	3280	1.01	0.0456	0.866	3.0	2.6	7.4	0.733	0.253	0.366	0.177	0.086	0.167	0.70		
	3280	1.10	0.0091	0.864	3.0	2.6	5.9	0.733	0.402	0.587	0.296	0.135	0.265	0.74		
	3280	1.20	0.0113	0.809	3.0	2.4	6.3	0.733	0.352	0.667	0.257	0.118	0.235	0.73		
	3280	1.30	0.0252	0.751	3.0	2.3	7.3	0.733	0.262	0.777	0.178	0.088	0.178	0.68		

[a] Used as reported without correction for hydrosilylation side reactions

Correction for side reactions will be carried out only for the data obtained from reference 9, since it is the only set for which values of r/r' can be determined with any reliability. The remaining data points had to be used as reported without any further correction for side reactions[17,22–24]. The data points which were corrected for side reactions are all for networks having a sol fraction $<7\%$. Also, it is worth noting that the values of ν_a, μ_a and T_e computed from branching theory are lower than the values which correspond to complete end-linking. These values are reduced, in general, by a factor of about 2 to 3. The results reported in the literature and those corrected for side reactions are reported in *Tables 1* and *2*, respectively, for the trifunctional networks. *Tables 3* and *4* present the corresponding results for the tetrafunctional networks.

Use of the phantom and the constrained-junction theory to interpret a wealth of experimental data leads to identification of the phantom modulus $[f^*]_{ph}$ at least approximately with the phenomenological constant $2C_1$[11–21]. Values of $[f^*]_{ph}$ calculated here, however, are two- to three-fold lower than the corresponding values of $2C_1$. This is presumably due to inherent inaccuracies, mentioned above, in determinations of the sol fraction. In any case, it is contrary to all experimental and theoretical assumptions where $[f^*]_{ph}$ [expressed by equation (23)], should hold for any network regardless of its functionality or the presence of defects (such as dangling chains, connected to the network at only one end).

For purposes of comparison, the results for trifunctional networks are shown in *Figure 1* with the same values of r that were used to obtain the structural parameters of the network without correction for side reactions[5,9]. Here, values of G are plotted against values of $\nu_a RT$, consistent with equation (3). The solid line represents theory according to which the ordinate should equal the abscissa in the affine limit, where $\kappa \to \infty$. The dashed line shows values of the phantom modulus $[f^*]_{ph}$ calculated from equation (23). At the lower degrees of crosslinking, values of G exceed those predicted by the theory. The data, however, do not unambiguously suggest any appreciable intercept that could be attributed to significant contributions from trapped entanglements. Hence, $G_e \approx 0$, and likewise the small-strain modulus G vanishes in the limit $\nu_a RT \to 0$. The interesting point here is that at intermediate values of $\nu_a RT$, there is a transition

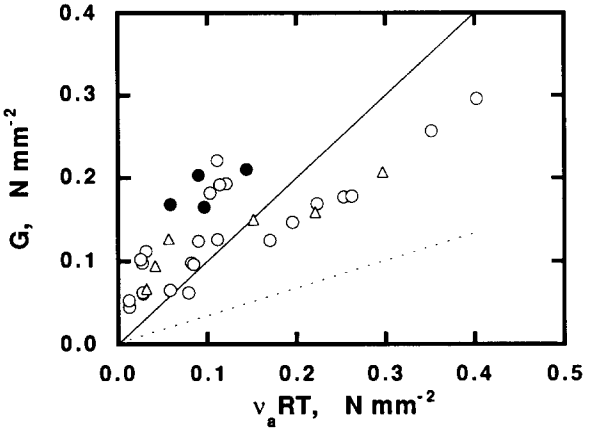

Figure 1 Modulus shown as a function of the affine modulus expected for the network active chain density ν_a. The solid line is for the affine modulus, and the dashed line for the phantom limit. The experimental data are for trifunctional PDMS model networks, as reported by Mark *et al.*[23] (△), Meyers[19] (●) and Macosko and Benjamin[9] (○)

Table 2 Elastomeric properties of the trifunctional PDMS networks with corrections for side reactions[a]

M_n (g mol^{-1})	r' [b]	ω_s	P'_{SiH}	v_2	φ	κ	$\nu_0 RT$ (N mm^{-2})	$\nu_a RT$ (N mm^{-2})	νRT (N mm^{-2})	G (N mm^{-2})	$[f^*]_{ph}$ (N mm^{-2})	$[f^*]_{\alpha\to 1}$ (N mm^{-2})	$G/\nu RT$
30000	1.09	0.0325	0.835	0.707	3.0	19.1	0.080	0.031	0.112	0.013	0.028	2.20	0.451
30000	1.21	0.0358	0.777	0.696	3.0	20.6	0.080	0.027	0.097	0.011	0.025	1.50	0.433
30000	1.29	0.0367	0.745	0.694	3.0	20.6	0.080	0.025	0.102	0.011	0.024	1.30	0.428
22400	1.00	0.0760	0.851	0.604	3.0	21.8	0.107	0.028	0.061	0.010	0.024	1.40	0.275
22400	1.00	0.0730	0.853	0.609	3.0	21.3	0.107	0.028	0.062	0.010	0.024	1.50	0.283
11400	0.91	0.0790	0.899	0.602	3.0	14.6	0.211	0.058	0.065	0.022	0.047	0.90	0.266
11400	1.00	0.0314	0.888	0.713	3.0	12.5	0.211	0.090	0.124	0.031	0.069	1.00	0.456
11400	1.11	0.0073	0.863	0.847	3.0	10.6	0.211	0.121	0.193	0.042	0.095	1.10	0.700
11400	1.21	0.0060	0.814	0.863	3.0	11.1	0.211	0.114	0.192	0.038	0.089	0.90	0.729
11400	1.31	0.0040	0.775	0.890	3.0	11.1	0.211	0.111	0.221	0.038	0.088	0.80	0.780
11400	0.99	0.0381	0.887	0.691	3.0	12.7	0.211	0.082	0.098	0.030	0.064	0.90	0.418
11400	0.99	0.0369	0.888	0.694	3.0	12.9	0.211	0.085	0.096	0.029	0.065	0.90	0.424
11400	1.11	0.0106	0.855	0.820	3.0	11.1	0.211	0.111	0.126	0.038	0.086	0.70	0.648
11400	1.34	0.0055	0.759	0.872	3.0	11.7	0.211	0.103	0.182	0.035	0.081	0.60	0.746
5430	0.99	0.1190	0.835	0.564	3.0	12.9	0.443	0.079	0.062	0.028	0.059	0.50	0.182
4190	0.99	0.0497	0.876	0.669	3.0	8.5	0.574	0.196	0.147	0.065	0.133	0.50	0.361
4190	1.15	0.0255	0.813	0.748	3.0	7.9	0.574	0.223	0.169	0.076	0.155	0.40	0.501
4190	1.25	0.0418	0.757	0.698	3.0	9.1	0.574	0.170	0.125	0.057	0.120	0.30	0.407
3280	1.01	0.0456	0.866	0.683	3.0	7.4	0.733	0.253	0.177	0.086	0.167	0.50	0.379
3280	1.10	0.0091	0.864	0.840	3.0	5.9	0.733	0.402	0.296	0.135	0.265	0.50	0.671
3280	1.20	0.0113	0.809	0.829	3.0	6.3	0.733	0.352	0.257	0.118	0.235	0.40	0.648
3280	1.30	0.0252	0.751	0.762	3.0	7.3	0.733	0.262	0.178	0.088	0.178	0.20	0.516

[a] The experimental results were obtained by Macosko and Benjamin[9]
[b] Corrected for hydrosilylation side reactions by a factor of $r'/r = 1/1.2$

Table 3 Elastomeric properties of the tetrafunctional PDMS networks

Source	M_n (g mol^{-1})	r^a	ω_s	P_{SiH}	v_2	φ_e	κ	v_0RT (N mm^{-2})	v_aRT (N mm^{-2})	G (N mm^{-2})	$[f^*]_{ph}$ (N mm^{-2})	$[f^*]_{\alpha\to 1}$ (N mm^{-2})	G/vRT	T_e	$2C_1$ (N mm^{-2})	$2C_2$ (N mm^{-2})
Mark and Sullivan[22]	45000	1.00	0.0750	0.788	0.603	3.2	22.3	0.053	0.021	0.068	0.008	0.018	3.26	0.278	0.038	0.030
	32900	1.00	0.0460	0.822	0.664	3.3	16.4	0.073	0.037	0.100	0.015	0.030	2.68	0.380	0.058	0.042
	25600	1.00	0.0170	0.881	0.774	3.5	11.9	0.094	0.067	0.140	0.028	0.053	2.10	0.571	0.084	0.055
	18500	1.00	0.0600	0.804	0.632	3.3	13.3	0.130	0.058	0.129	0.023	0.045	2.23	0.324	0.089	0.040
	9500	1.00	0.0300	0.849	0.716	3.4	8.0	0.253	0.153	0.217	0.062	0.109	1.42	0.466	0.167	0.050
	4700	1.00	0.0340	0.841	0.704	3.4	5.8	0.512	0.294	0.384	0.119	0.192	1.31	0.439	0.353	0.031
	4000	1.00	0.0210	0.897	0.808	3.5	4.5	0.601	0.456	0.416	0.195	0.298	0.91	0.625	0.395	0.021
Llorente and Mark[24]	18500	1.00	0.0740	0.789	0.607	3.3	14.3	0.130	0.051	0.139	0.020	0.039	2.73	0.280	0.096	0.043
	18500	1.00	0.0740	0.789	0.607	3.3	14.3	0.130	0.051	0.132	0.020	0.039	2.59	0.280	0.089	0.043
	18500	1.00	0.0740	0.789	0.607	3.3	14.3	0.130	0.051	0.129	0.020	0.039	2.53	0.280	0.089	0.040
Llorente and Mark[25]	11300	1.00	0.0050	0.931	0.870	3.6	7.0	0.213	0.183	0.279	0.082	0.137	1.53	0.744	0.196	0.083
	11300	1.00	0.0060	0.925	0.858	3.6	7.1	0.213	0.179	0.284	0.079	0.134	1.59	0.723	0.169	0.115
	11300	1.00	0.0040	0.938	0.882	3.6	6.9	0.213	0.186	0.275	0.084	0.140	1.47	0.769	0.199	0.076
	11300	1.33	0.0030	0.733	0.900	3.4	7.9	0.213	0.157	0.275	0.064	0.119	1.75	0.802	0.188	0.092
	11300	1.33	0.0050	0.724	0.872	3.3	8.2	0.213	0.149	0.276	0.060	0.113	1.85	0.748	0.178	0.098
	11300	1.33	0.0040	0.728	0.885	3.3	8.1	0.213	0.153	0.285	0.062	0.116	1.86	0.772	0.165	0.120
Valles and Macosko[7]	11600	1.00	0.0000	1.000	1.000	4.0	6.2	0.207	0.209	0.259	0.104	0.163	1.24	1.000		
	11600	1.00	0.0000	1.000	1.000	4.0	6.1	0.207	0.218	0.255	0.109	0.169	1.17	1.000		
Meyers[19]	21600	1.12	0.0049	0.839	0.871	3.5	10.3	0.111	0.089	0.240	0.038	0.071	2.70	0.747	0.142	0.098
	15200	1.00	0.0081	0.914	0.837	3.6	8.4	0.158	0.128	0.258	0.056	0.098	2.01	0.684		
	11100	1.10	0.0012	0.880	0.934	3.6	6.8	0.217	0.194	0.294	0.086	0.147	1.51	0.868	0.207	0.087
	8800	1.01	0.0049	0.923	0.871	3.6	6.2	0.273	0.234	0.328	0.104	0.170	1.40	0.746	0.244	0.084
Macosko and Benjamin[9]	30000	1.11	0.0441	0.760	0.670	3.3	16.3	0.080	0.039	0.131	0.015	0.032	3.37	0.389		
	30000	1.20	0.0242	0.742	0.739	3.3	14.9	0.080	0.046	0.146	0.018	0.037	3.20	0.508		
	30000	1.32	0.0213	0.694	0.753	3.3	15.3	0.080	0.044	0.144	0.017	0.036	3.28	0.532		
	22400	1.03	0.0401	0.811	0.682	3.3	13.2	0.107	0.058	0.114	0.023	0.045	1.97	0.408		
	22400	1.11	0.0161	0.807	0.780	3.4	11.6	0.107	0.073	0.176	0.030	0.058	2.42	0.580		
	22400	1.21	0.0173	0.750	0.773	3.3	12.3	0.107	0.067	0.160	0.027	0.053	2.39	0.569		
	22400	1.30	0.0162	0.710	0.780	3.3	12.6	0.107	0.064	0.151	0.025	0.051	2.35	0.581		
	11400	1.00	0.0157	0.884	0.783	3.5	7.9	0.211	0.153	0.205	0.064	0.112	1.34	0.583		
	11400	1.06	0.0034	0.892	0.891	3.6	7.1	0.211	0.182	0.250	0.080	0.136	1.38	0.785		
	11400	1.10	0.0025	0.868	0.906	3.5	7.1	0.211	0.182	0.291	0.079	0.137	1.60	0.814		
	11400	1.13	0.0032	0.842	0.895	3.5	7.3	0.211	0.175	0.262	0.075	0.132	1.50	0.791		
	11400	1.13	0.0860	0.712	0.591	3.2	12.4	0.211	0.069	0.093	0.026	0.051	1.35	0.249		
	11400	1.17	0.0040	0.812	0.883	3.4	7.5	0.211	0.169	0.295	0.071	0.127	1.74	0.770		
	11400	1.18	0.0014	0.823	0.929	3.5	7.2	0.211	0.180	0.303	0.077	0.136	1.68	0.859		
	11400	1.19	0.0070	0.787	0.849	3.4	7.9	0.211	0.155	0.221	0.064	0.116	1.43	0.705		

11400	1.20	0.0029	0.800	0.900	3.4	7.5	0.211	0.171	0.268	0.072	0.129	1.57	0.801		
11400	1.30	0.0016	0.755	0.926	3.4	7.6	0.211	0.167	0.276	0.068	0.126	1.66	0.853		
11400	1.33	0.0078	0.716	0.843	3.3	8.5	0.211	0.140	0.228	0.056	0.105	1.63	0.693		
4190	1.00	0.0083	0.912	0.838	3.5	4.5	0.574	0.460	0.343	0.200	0.304	0.75	0.678		
4190	1.10	0.0052	0.851	0.870	3.5	4.5	0.574	0.458	0.360	0.195	0.305	0.79	0.738		
4190	1.20	0.0041	0.794	0.886	3.4	4.7	0.574	0.443	0.461	0.184	0.296	1.04	0.768		
4190	1.31	0.0037	0.739	0.895	3.4	4.8	0.574	0.421	0.426	0.170	0.282	1.01	0.785		
29200	1.10	0.0288	0.787	0.720	3.3	14.8	0.082	0.046	0.146	0.018	0.037	3.17	0.475		
21600	0.97	0.0059	0.950	0.859	3.6	9.7	0.111	0.094	0.206	0.042	0.075	2.20	0.725		
21600	0.97	0.0048	0.957	0.872	3.7	9.6	0.111	0.096	0.230	0.044	0.077	2.40	0.749		
21000	1.10	0.0062	0.846	0.856	3.5	10.3	0.115	0.089	0.225	0.038	0.071	2.54	0.720		
11600	1.20	0.0041	0.794	0.882	3.4	7.8	0.207	0.158	0.307	0.065	0.119	1.94	0.767		
11600	1.20	0.0048	0.790	0.873	3.4	7.9	0.207	0.155	0.293	0.064	0.117	1.89	0.750		
11600	1.20	0.0072	0.781	0.847	3.4	8.1	0.207	0.147	0.274	0.060	0.111	1.86	0.701		
11400	1.25	0.0077	0.753	0.843	3.4	8.3	0.211	0.144	0.241	0.058	0.108	1.67	0.693		
3010	1.20	0.0015	0.810	0.931	3.5	3.8	0.799	0.659	0.500	0.279	0.426	0.76	0.857		
1800	1.20	0.0056	0.787	0.875	3.4	3.1	1.337	1.011	0.890	0.417	0.603	0.88	0.732		
Granick *et al.*[8]															

[a] Used as reported without correction for hydrosilylation side reactions

toward the phantom limit of the modulus. This trend will be explored in greater detail below.

If side reactions resulting in losses of Si-H groups[11] are accounted for, then values of the effective stoichiometric ratio r' should be lower than the initial value r. *Figure 2* is a plot of G against $\nu_a RT$ for trifunctional networks, where the effective values of r' ($r/r' \approx 1.2$) have been used to obtain the structural parameters of the network. Better agreement between theory and experiment is now observed. The solid line represents the upper bound of theory (the affine modulus), as in equation (3). The results suggest a linear relationship of unit slope, within the limits of experimental error. Correspondence of experimental values of G with the calculated values of $\nu_a RT$ is particularly close at low values of $\nu_a RT$. Any entanglements latent in the polymer prior to crosslinking do not seem to contribute much to the modulus after crosslinking. The enhancement of $[f^*]$ at $\alpha \rightarrow 1$ has been observed to vanish upon swelling, suggesting it is due to difficulties in reaching elastic equilibrium when the network chains are very long. Thus, the behaviour observed appears to be within the limits of the constrained-junction theory of Flory and Erman[33–36].

It is important to emphasize the non-equivalence of ν and ν_a. Values of the effective number of strands ν (relevant to the theory of elasticity) have been calculated using branching theory and equation (28). In *Figure 3*,

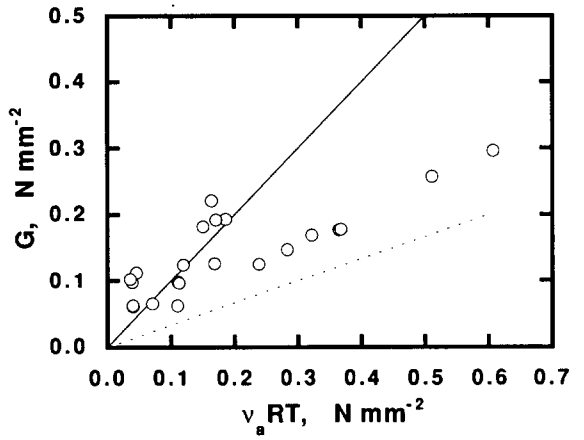

Figure 2 The comparisons made in *Figure 1*, but with correction for side reactions in the hydrosilylation cure as outlined in the text. The experimental data are those reported by Macosko and Benjamin[9]

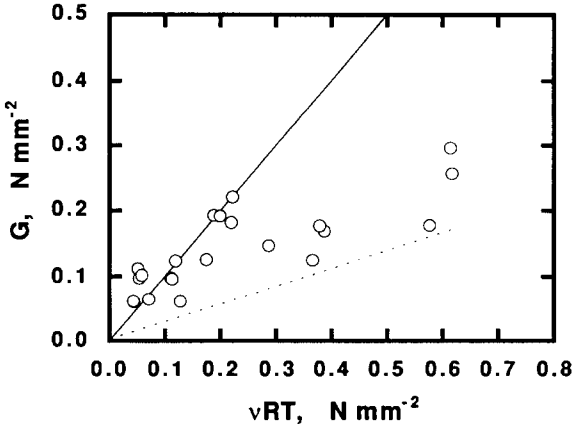

Figure 3 The comparisons made in *Figure 2*, but shown as a function of the effective chain density ν, calculated according to equation (28)

Table 4 Elastomeric properties of the tetrafunctional PDMS networks with corrections for side reactions[a]

M_n (g mol^{-1})	r' [b]	ω_s	P'_{SiH}	v_2	φ_e	κ	$\nu_0 RT$ (N mm^{-2})	$\nu_e RT$ (N mm^{-2})	G (N mm^{-2})	$[f^*]_{ph}$ (N mm^{-2})	$[f^*]_{\alpha\to 1}$ (N mm^{-2})	$G/\nu RT$	T_e
30000	1.11	0.0441	0.760	0.670	3.3	16.3	0.080	0.039	0.131	0.015	0.032	3.37	0.389
30000	1.20	0.0242	0.742	0.739	3.3	14.9	0.080	0.046	0.146	0.018	0.037	3.20	0.508
30000	1.32	0.0213	0.694	0.753	3.3	15.3	0.080	0.044	0.144	0.017	0.036	3.28	0.532
22400	1.03	0.0401	0.811	0.682	3.3	13.2	0.107	0.058	0.114	0.023	0.045	1.97	0.408
22400	1.11	0.0161	0.807	0.780	3.4	11.6	0.107	0.073	0.176	0.030	0.058	2.42	0.580
22400	1.21	0.0173	0.750	0.773	3.3	12.3	0.107	0.067	0.160	0.027	0.053	2.39	0.569
22400	1.30	0.0162	0.710	0.780	3.3	12.6	0.107	0.064	0.151	0.025	0.051	2.35	0.581
11400	1.00	0.0157	0.884	0.783	3.5	7.9	0.211	0.153	0.205	0.064	0.112	1.34	0.583
11400	1.10	0.0025	0.868	0.906	3.5	7.1	0.211	0.182	0.291	0.079	0.137	1.60	0.814
11400	1.13	0.0032	0.842	0.895	3.5	7.3	0.211	0.175	0.262	0.075	0.132	1.50	0.791
11400	1.13	0.0860	0.712	0.591	3.2	12.4	0.211	0.069	0.093	0.026	0.051	1.35	0.249
11400	1.17	0.0040	0.812	0.883	3.4	7.5	0.211	0.169	0.295	0.071	0.127	1.74	0.770
11400	1.18	0.0014	0.823	0.929	3.5	7.2	0.211	0.180	0.303	0.077	0.136	1.68	0.859
11400	1.19	0.0070	0.787	0.849	3.4	7.9	0.211	0.155	0.221	0.064	0.116	1.43	0.705
11400	1.20	0.0029	0.800	0.900	3.4	7.5	0.211	0.171	0.268	0.072	0.129	1.57	0.801
11400	1.30	0.0016	0.755	0.926	3.4	7.6	0.211	0.167	0.276	0.068	0.126	1.66	0.853
11400	1.33	0.0078	0.716	0.843	3.3	8.5	0.211	0.140	0.228	0.056	0.105	1.63	0.693
4190	1.00	0.0083	0.912	0.838	3.5	4.5	0.574	0.460	0.343	0.200	0.304	0.75	0.678
4190	1.10	0.0052	0.851	0.870	3.5	4.5	0.574	0.458	0.360	0.195	0.305	0.79	0.738
4190	1.20	0.0041	0.794	0.886	3.4	4.7	0.574	0.443	0.461	0.184	0.296	1.04	0.768
4190	1.31	0.0037	0.739	0.895	3.4	4.8	0.574	0.421	0.426	0.170	0.282	1.01	0.785

[a] The experimental results were obtained by Macosko and Benjamin[9]
[b] Corrected for hydrosilylation side reactions by a factor of $r'/r = 1/1.2$

dependence of G on the presumably more-nearly correct value νRT is demonstrated. Near-perfect agreement between theory and experiment is observed at lower values of νRT, within limits set by the scattering of the data. The results so presented are well interpreted using the constrained-junction theory and underscore the importance of distinguishing between ν_a and ν.

Another property that is of interest is the ratio $G/\nu RT$ of the small-strain modulus to the theoretical value of the affine modulus, in equation (24). It is clear that its maximum expected value is unity. The dependence of these values on νRT is shown in *Figure 4*. The three points that show the largest increase above unity are those for networks having $M_n = 30000$ g mol^{-1}. Such values could be due mainly to difficulties in reaching elastic equilibrium when the network chains are very long, or to higher slopes in the Mooney–Rivlin extrapolations[26]. This suggestion is supported by the fact that the values of G are higher than those for networks having $M_n = 22400$ g mol^{-1}, which is the reverse of what is expected. The fact that almost all values of $G/\nu RT$ are equal or less than unity suggests that trapped entanglements in these networks do not play a major role at elastic equilibrium.

The results presented in *Figures 1–3* show an unmistakable departure in the values of G from the upper affine bound as νRT increases. Again, actual values of G predicted by the constrained-junction theory should fall below the upper bound even at small strain. Such decreases in values of G with increase in crosslink density are expected because of the decrease in chain interpenetration as the network chain length decreases. In previous comparisons of experiment with theory, neglect of this factor could have led to incorrect inferences. It is probably inappropriate to make the contributions

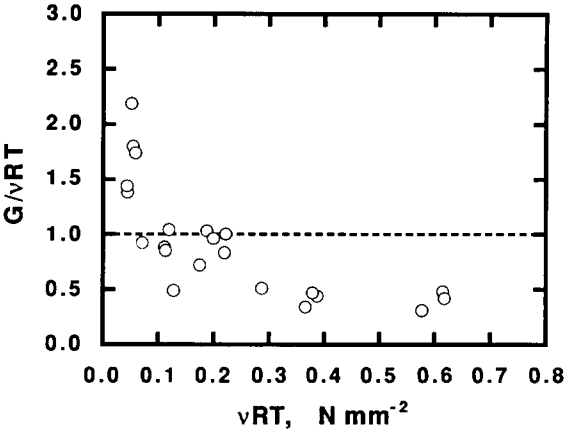

Figure 4 Values of the ratio $G/\nu RT$ of the experimental modulus to the calculated affine modulus for the trifunctional PDMS networks. The dashed line is for the affine modulus, and the experimental data[9] are for trifunctional PDMS model networks

from constraints on the fluctuations a constant fraction of the reduced stress regardless of the degree of crosslinking. In fact, the constrained-junction theory allows for a decrease in the degree of interpenetration as the network chain length decreases[33–36]. In the above analysis, a substantial intercept of magnitude comparable to those obtained in previous studies would be obtained only upon extrapolation through the data in the region where the affine to phantom transition ensues. This would not be consistent with the curves consisting of two discernible segments.

Also of interest are suggestions that topological entanglements contribute to the small-strain modulus at

small crosslink densities, and that direct proportionality to chemical crosslink density is found only at high degrees of crosslinking[20]. Such conclusions could be due to neglect of the fact that at the high temperatures employed for hydrosilylation, network imperfections are probably enhanced, as already mentioned. Any increase in modulus from such entanglements would be expected to be largest at the lower degrees of crosslinking, however, and this was not the case[20].

Intuitively, and according to equations (9) and (10), the modulus $[f^*]_c$ due to constraints should increase with increase in the number of junctions μ (i.e. with the degree of crosslinking). However, further increase in the degree of crosslinking would lead to lower values of the degree of interpenetration between chains and junctions. Eventually, this will decrease $[f^*]_c$ through decrease in κ, as predicted by equation (19). Results discussed below seem to be consistent with this expectation. Thus, the transition proposed as being from the plateau modulus of PDMS to the range of direct proportionality could alternatively be interpreted as a transition between the affine and phantom limits of deformation with increase in the degree of crosslinking.

The results of calculations of the modulus and related quantities from the constrained-junction theory[34-36] are illustrated in *Figure 5*. The small-deformation modulus $[f^*]_{\alpha\to 1}$, calculated from equation (9), is shown as a function of the affine modulus expected for the effective network chain density ν. The dotted-and-dashed line represents the upper bound (the affine limit), and the dashed line the phantom modulus [as obtained from equation (5)]. The dotted line represents the contribution to the modulus from constraints on the junction fluctuations, calculated according to equations given elsewhere[34-36]. As expected, values of $[f^*]_{\alpha\to 1}$ are lower than the theoretical affine modulus. It is apparent that the theory accounts, at least qualitatively, for these experimental observations.

It can be argued that if trapped entanglements are operative, they should contribute to the modulus at all deformations, i.e. to both the phantom modulus $[f^*]_{ph}$ and the shear modulus G. Therefore, *Figure 6* was prepared to show values of $2C_1$ as a function of $[f^*]_{ph} + G_e T_e$ for the results[23] reported on the trifunctional PDMS networks. The solid line represents the assumption that entanglements contribute to the large-strain modulus and is seen to give a poor fit of the experimental results.

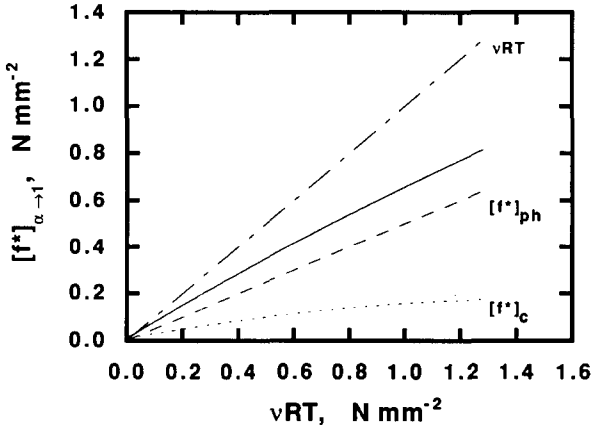

Figure 5 Theoretical values of the small-deformation moduli ($\alpha\to 1$) as obtained from the constrained-junction model and related quantities, shown as a function of the affine modulus expected for the effective network chain density ν. The solid line represents the modulus at $\alpha\to 1$, the dotted-and-dashed line is for the affine modulus, and the dashed line is for the phantom limit. The dotted curve represents the contribution from the constraints on the junctions

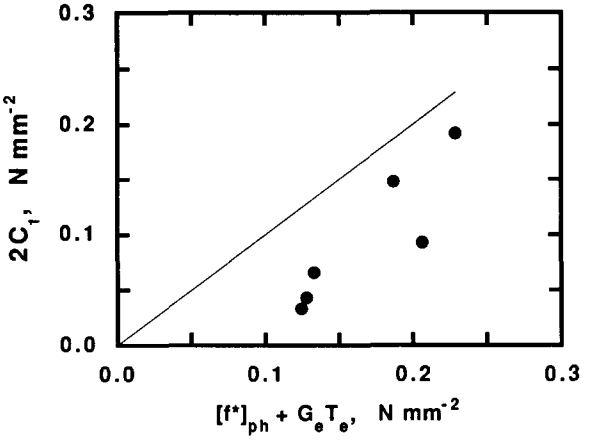

Figure 6 The Mooney–Rivlin estimate of the high-deformation modulus shown as a function of the phantom modulus as augmented by a term for contributions from trapped entanglements. The solid line represents equivalence of the two types of modulus. The elastomers are model trifunctional networks of PDMS as reported by Mark *et al.*[23]

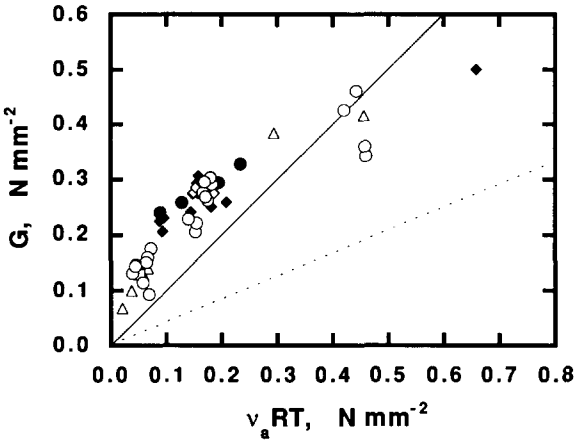

Figure 7 The comparisons made in *Figure 1*, but for tetrafunctional PDMS networks as reported by Mark and Sullivan[22] (△), Llorente and Mark[24] (□), Llorente and Mark[25] (◇), Meyers *et al.*[17] (●) Granick *et al.*[8] (◆) and Macosko and Benjamin[9] (○)

Comparisons for tetrafunctional networks are given in *Figure 7*, which shows the change of G with values of $\nu_a RT$ calculated from sol fractions. Again, there does not seem to be an appreciable intercept that could be attributed to significant contributions from trapped entanglements. There does seem, however, to be a transition towards the phantom limit at intermediate values of $\nu_a RT$. *Figure 8* demonstrates that there is better agreement between theory and experiment when side reactions of the Si-H group are taken into account by using the corrected value r' to obtain the network parameters. (As mentioned earlier, values of ν_a were used as approximate substitutes for ν.) The departure observed at low values of $\nu_a RT$ could be due primarily to inaccuracies in defining the initial stoichiometry. This possible source of error was discussed in a similar investigation[38] that used the same starting materials as

the earlier study[9]. The tetrafunctional crosslinking agent was found to have an average functionality of 3.5 and a purity of ~90%[38]. The resulting uncertainty in the network structural parameters illustrates a major problem in the study of rubber elasticity, particularly in regard to testing the various theories. An additional problem could be difficulties arising from inhomogeneities in the crosslinking process, as has been pointed out elsewhere[50].

One way to avoid some of the cited difficulties in obtaining accurate values of the network structural parameters is to plot $G \approx 2C_1 + 2C_2$ against $2C_1 \approx [f^*]_{ph}$. According to the Flory–Erman theory[33–36], $[f^*]_{ph}$ is proportional to the effective interconnectivity of the network, and can therefore be used to define an effective number of chains ν and junctions μ, regardless of junction functionality and incompleteness of the formation reaction. The data obtained from the literature are plotted in *Figures 9* and *10* for trifunctional[23] and tetrafunctional[17,22,24] networks, respectively. In each of these two figures, the dashed line represents the lower bound of the theory (the phantom limit), and the solid line approximates the upper bound (the affinely deforming network). The latter was calculated from equation (26)[46] which, for an imperfect network, gives:

$$[f^*]_{aff} = \nu RT = 2\xi RT = 2(2C_1) \qquad (40)$$

The results are well represented within the two limits of deformation. Again, as the degree of crosslinking is increased, a transition toward the lower bound (the phantom limit) is observed. This is expected, since the constraints on the fluctuations of the junctions vanish with an increase in either the degree of crosslinking or the deformation. The results thus appear to be in accord with the main premises of the constrained-junction theory[46]. Additional improvements in the agreement between theory and experiment might be obtained by employing the recently proposed, and more realistic, constrained-chain theory[51].

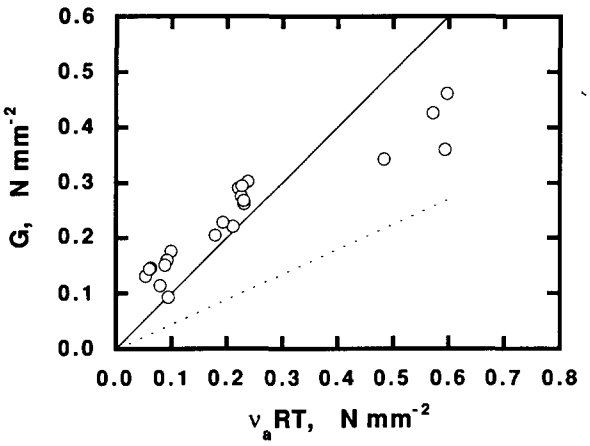

Figure 8 The comparisons made in *Figure 2*, but for tetrafunctional PDMS networks as reported by Macosko and Benjamin[9]

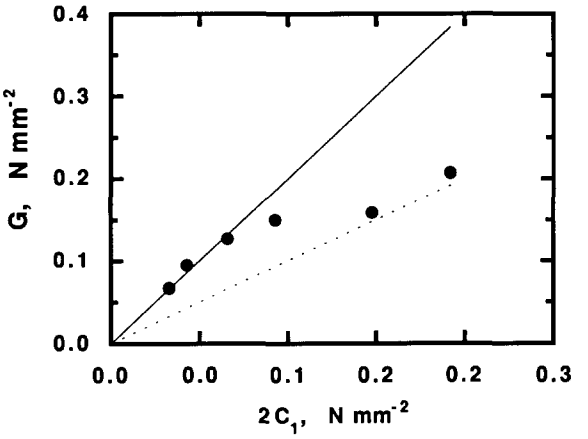

Figure 9 Modulus shown as a function of the Mooney–Rivlin estimate of the high-deformation modulus. The solid line is for the affine limit for an imperfect network as approximated by $2(2C_1)$, calculated according to equation (40). The dashed line is for the phantom modulus approximated by $2C_1$ itself. The experimental points are for trifunctional networks as reported by Mark *et al.*[23]

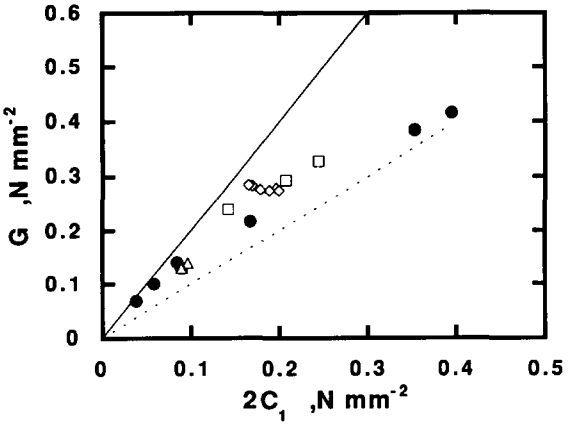

Figure 10 The comparisons made in *Figure 9*, but for tetrafunctional networks as reported by Llorente and Mark[24] (□), Llorente and Mark[25] (◇) and Meyers *et al.*[17] (●)

ACKNOWLEDGEMENT

It is a pleasure to acknowledge the financial support by the National Science Foundation through Grant DMR 89-18002 (Polymers Program, Division of Materials Research).

REFERENCES

1 James, H. M. and Guth, E. *J. Chem. Phys.* 1947, **15**, 669
2 Flory, P. J. 'Principles of Polymer Chemistry', Cornell University Press· Ithaca, 1953
3 Treloar, L. R. G. 'The Physics of Rubber Elasticity', 3rd Edn, Clarendon Press, Oxford, 1975
4 Mark, J. E. and Erman, B. 'Rubberlike Elasticity. A Molecular Primer', Wiley-Interscience, New York, 1988
5 Gottlieb, M., Macosko, C. W., Benjamin, G. S., Meyers, K. O. and Merrill, E. W. *Macromolecules* 1981, **14**, 1039
6 Valles, E. M. and Macosko, C. W. *Rubber Chem. Technol.* 1976, **49**, 132
7 Valles, E. M. and Macosko, C. W. *Macromolecules* 1979, **12**, 673
8 Granick, S., Pedersen, S., Nelb, G. W., Ferry, J. D. and Macosko, C. W. *J. Polym. Sci., Polym. Phys. Edn* 1981, **19**, 1745
9 Macosko, C. W. and Benjamin, G. S. *Pure Appl. Chem.* 1981, **53**, 1505
10 Gottlieb, M., Macosko, C. W. and Lepsch, T. P. *J. Polym. Sci., Polym. Phys. Edn* 1981, **19**, 1603
11 Macosko, C. W. and Saam, J. C. *Polym. Bull.* 1987, **18**, 463
12 Aranguren, M. I. and Macosko, C. W. *Macromolecules* 1988, **21**, 2484
13 Ferry, J. D. 'Viscoelastic Properties of Polymers', 2nd Edn, Wiley, New York, 1979
14 Langley, N. P. *Macromolecules* 1968, **1**, 348
15 Dossin, L. M. and Graessley, W. W. *Macromolecules* 1979, **12**, 123
16 Pearson, D. S. and Graessley, W. W. *Macromolecules* 1980, **13**, 1001

17 Meyers, K. O., Bye, M. I. and Merrill, E. W. *Macromolecules* 1980, **13**, 1045
18 Kirk, K. A., Bidstrup, S. S., Merrill, E. W. and Meyers, K. O. *Macromolecules* 1982, **15**, 112
19 Meyers, K. O. *PhD Thesis* Massachusetts Institute of Technology, 1980
20 Oppermann, W. and Rennar, N. *Prog. Coll. Polym. Sci.* 1987, **75**, 49
21 Edwards, S. E. and Vilgis, T. A. *Rep. Prog. Phys.* 1988, **51**, 243
22 Mark, J. E. and Sullivan, J. L. *J. Chem. Phys.* 1977, **66**, 1006
23 Mark, J. E., Rahalkar, R. R. and Sullivan, J. L. *J. Chem. Phys.* 1979, **70**, 1749
24 Llorente, M. A. and Mark, J. E. *J. Chem. Phys.* 1979, **71**, 682
25 Llorente, M. A. and Mark, J. E. *Macromolecules* 1980, **13**, 681
26 Queslel, J. P. and Mark, J. E. *Adv. Polym. Sci.* 1985, **17**, 229
27 Erman, B., Wagner, W. and Flory, P. J. *Macromolecules* 1980, **13**, 1554
28 Erman, B. and Flory, P. J. *Macromolecules* 1982, **15**, 806
29 Flory, P. J. and Erman, B. *J. Polym. Sci., Polym. Phys. Edn* 1984, **22**, 49
30 Sharaf, M. A. and Mark, J. E. *Polym. Mater. Sci. Eng. Prepr.* 1990, **62**, 644
31 Sharaf, M. A. and Mark, J. E. *J. Polym. Sci., Polym. Phys. Edn* submitted
32 Ronca, G. and Allegra, G. *J. Chem. Phys.* 1975, **63**, 4990
33 Flory, P. J. *Proc. R. Soc. London A* 1976, **351**, 351
34 Flory, P. J. *J. Chem. Phys.* 1977, **66**, 5720
35 Erman, B. and Flory, P. J. *J. Chem. Phys.* 1978, **68**, 5363
36 Flory, P. J. and Erman, B. *Macromolecules* 1982, **15**, 800
37 Sundar, K. V., Coyne, L., Chambon, F., Gottlieb, M. and Winter, H. M. *Polymer* 1989, **30**, 2222
38 Gent, A. N. and Tobias, R. H. in 'Elastomers and Rubber Elasticity' (Eds J. E. Mark and J. Lal), American Chemical Society, Washington, DC, 1982
39 Leung, Y. and Eichinger, B. E. *J. Chem. Phys.* 1984, **80**, 3885
40 Mooney, M. *J. Appl. Phys.* 1940, **1**, 582
41 Rivlin, R. S. *Phil. Trans. R. Soc. London A* 1948, **241**, 379
42 Scanlan, J. *J. Polym. Sci.* 1960, **43**, 501
43 Case, L. C. *J. Polym. Sci.* 1960, **45**, 397
44 Graessley, W. W. *Macromolecules* 1975, **8**, 186
45 Pearson, D. S. and Graessley, W. W. *Macromolecules* 1978, **11**, 528
46 Flory, P. J. *Macromolecules* 1982, **15**, 99
47 Macosko, C. W. and Miller, D. R. *Macromolecules* 1976, **9**, 199
48 Miller, D. R., Valles, E. M. and Macosko, C. W. *Polym. Eng. Sci.* 1979, **19**, 272
49 Erman, B. and Mark, J. E. *Macromolecules* 1987, **20**, 11
50 Falender, J. R., Yeh, G. S. Y. and Mark, J. E. *Macromolecules* 1979, **12**, 1207
51 Erman, B. and Monnerie, L. *Macromolecules* 1989, **22**, 3342